Processes controlling seasonality and spatial distribution of *Centropages typicus*: a modeling study in the Gulf of Maine/ Georges Bank region

CHRISTOPH STEGERT*, RUBAO JI, NA LI AND CABELL S. DAVIS

BIOLOGY, WOODS HOLE OCEANOGRAPHIC INSTITUTION, 45 WATER ST REDFIELD 2-14, WOODS HOLE, MA 02543, USA

*CORRESPONDING AUTHOR: cstegert@whoi.edu

Copepod populations in the Gulf of Maine/Georges Bank region are dominated by warm water species in late summer/autumn, which are specifically adapted to lower food conditions and higher temperatures and metabolic costs. Better knowledge of their physiological processes and behavior is needed to estimate the impact of changes in environmental conditions on their seasonality and spatial distribution. We investigated the population dynamics of the warm water species *Centropages typicus* in this region using a copepod population model coupled with a three-dimensional ecosystem model. Although growth and development of copepods are well-investigated processes and well represented in population models, the importance of other life-history traits (e.g. cannibalism, feeding and migration strategies) and their impact on seasonal dynamics and spatial distributions are recognized but difficult to quantify. In this study, species-specific life-history traits were included to investigate their influence on the spatio-temporal patterns. The results confirmed our assumption that cannibalism is a possible constraint controlling the abundances on Georges Bank. Omnivorous feeding by *C. typicus* on both phytoplankton and microzooplankton is important for maintaining the population in the deeper basins, while vertical aggregation in zones of high-food concentration is a secondary mechanism sustaining the population in low-food seasons. Finally, advective influx from the upstream region on the Scotian Shelf is critical in sustaining the Gulf of Maine population.

KEYWORDS: *Centropages typicus*; copepod population model; life-history strategy; cannibalism; vertical migration; Gulf of Maine

INTRODUCTION

Copepods are abundant throughout the world oceans and serve as major food source for higher trophic levels, including larval and juvenile fish species (Lough *et al.*, 2005; Voss *et al.*, 2009). Being present in various ecosystems, different copepod species have developed life-history strategies distinct from each other depending on the environmental conditions (e.g. Peterson, 2001; Niehoff, 2007; Kiørboe, 2008). While some species are adapted to specific environmental conditions, others can survive in a wider range of conditions. To better quantify their role in the food web in relation to fish populations, it is important to understand how the characteristic traits

of copepod species influence their population dynamics.

Centropages typicus is widespread in the North Atlantic Ocean and is among the most abundant copepod species in this area with high abundances in shelf regions between 35 and 60°N (Continuous Plankton Recorder Survey Team, 2004). Spatially, *C. typicus* is more abundant in the warmer surface layer as well as in near-shore regions (Clarke, 1933; Davis, 1987; Durbin and Kane, 2007), but less abundant in deep waters (e.g. deep basins in the Gulf of Maine and slope waters). In an analysis of a large Continuous Plankton Recorder (CPR) data set for the North Atlantic Ocean, Beaugrand *et al*. (Beaugrand *et al.*, 2007) found that the highest abundances occur at temperatures of ∼17°C, while mean abundances are low at temperatures <11°C. A similar pattern can be found in the MARMAP/ECOMON[1] data set (Sherman, 1980; Kane, 2007) for the Gulf of Maine/Georges Bank (GoM/GB) region, where highest abundances are found between 15 and 18°C and lowest abundances occurred at temperatures <7°C (Fig. 1). This temperature preference results in a seasonal peak in October to November, shortly after the temperature in the upper layers reaches its maximum of 16−17°C and decreases in December as temperatures decline to 8−10°C (Durbin and Kane, 2007). From the MARMAP/ECOMON data set no clear relationship between *C. typicus* and chlorophyll concentration or salinity was found (Fig. 1). *Centropages typicus* is somehow able to thrive during the warm season in a relatively low-food environment (<1 mg Chl m^{-3} from summer to winter except at the subsurface maximum layer, where concentrations can reach up to 1.5 mg Chl m^{-3}). This adaptation suggests a life-history strategy that is different from the cold water species in the region, including *Calanus finmarchicus*, *Pseudocalanus* sp. or *Temora* sp., which have peak abundances following the spring phytoplankton bloom (Davis, 1987; Durbin and Casas, 2006).

This analysis leads to some key questions that need to be addressed for a better understanding of processes controlling copepod population dynamics in a shelf system such as the Gulf of Maine, including: (i) which species-specific processes are responsible for shaping the seasonality of *C. typicus*? (ii) what mechanisms exist to build a high population size at lower food concentrations in autumn? and (iii) what causes the observed

horizontal and vertical gradients in abundance within the Gulf of Maine?

To address these questions, we investigated key mechanisms controlling the seasonal and spatial distribution of *C. typicus* in the GoM/GB region using a copepod population model embedded into a three-dimensional model. In an earlier study, Ji *et al*. (Ji *et al.*, 2009) compared the annual development, fecundity and mortality of the species *Pseudocalanus* sp., *C. typicus* and *C. hamatus*. Using a single species model, they found that: (i) changing the species-specific development and fecundity parameterization from *Pseudocalanus* to *C. typicus*, keeping the same temperature-dependent mortality, resulted in a significant increase in population size; (ii) a higher baseline egg mortality rate for *C. typicus* (due to a broadcast spawning strategy) generated an annual cycle similar to *Pseudocalanus* sp. despite changes in physiological parameters. They concluded that the annual development is very sensitive to mortality, and that additional population dynamic processes needed to be incorporated into the model.

In this paper, we examine the sensitivity of formulations for parameterization in the model and test different behavioral and physiological processes. We then compare simulated abundances to observations to examine possible processes responsible for the observed patterns. Specifically, in addition to the basic processes of development, reproduction and mortality, we quantitatively examine the effects of temperature-dependent mortality, omnivorous feeding and cannibalism, vertical aggregation and advection as factors influencing the characteristic seasonal and spatial patterns of *C. typicus* in the GoM/GB region.

METHOD

We use the three-dimensional high-resolution physical model FVCOM, which is a prognostic, unstructured-grid, *F*inite-*V*olume *C*oastal *O*cean *M*odel. The hydrodynamics model (Chen *et al.*, 2003; 2007) was previously coupled to a four-compartment [nitrogen-phytoplankton-(micro) zooplankton-detritus, NPZD] lower trophic food web model (to supply food for copepods) and a stage structured concentration-based copepod population dynamics model (Hu *et al.*, 2008a).

The nitrogen-based NPZD model contains key aspects of lower trophic-level food web dynamics and is used to provide the prey concentration for the modeled copepod species. The model captures the major seasonal and spatial distributions of nutrient and phytoplankton dynamics across the GoM/GB region as a function of local and remote forcing. The Z component of this

---

[1]The MARMAP/ECOMON data set used here includes stage-specific C. *typicus* abundances from the Marine Resources Monitoring, Assessment and Prediction program and the ECOsystem MONitoring program by the National Oceanic and Atmospheric Administration (NOAA).
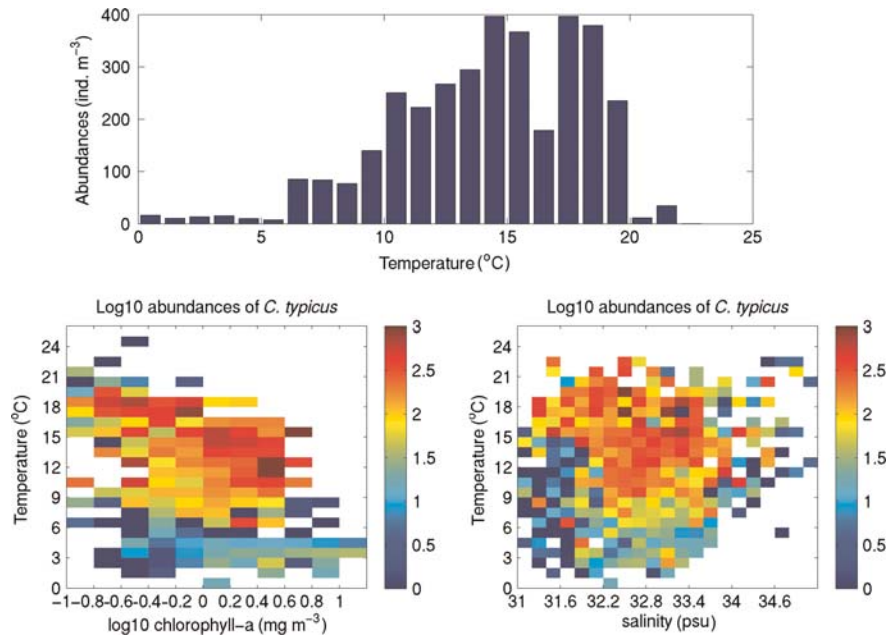
Fig. 1. Abundance of *Centropages typicus* in the Gulf of Maine/Georges Bank region in relation to environmental characteristics. Upper: surface temperature, lower left: temperature and chlorophyll-*a* surface concentration, lower right: surface temperature and salinity. Abundances are vertical averages over the upper 200 m in Log_{10} (ind. m^{-3}).

model is considered to be microzooplankton which responds rapidly to changes in phytoplankton. Further details on FVCOM and the NPZD model are presented in Ji *et al.* (Ji *et al.*, 2008a, b, 2009). Atmospheric forcing data (such as surface wind stress and heat flux) were provided by an atmospheric mesoscale model (MM5), while the FVCOM model was driven by realistic surface and boundary forcing with assimilation of satellite/buoy data for the year 1999. The initializing fields are based on climatological data as described in Ji *et al.* (Ji *et al.*, 2008a).

The four-stage (egg-nauplii-copepodite-adult) mean-age model (Hu *et al.*, 2008a) was used to simulate the population dynamics of *C. typicus*. This model was tested in a zero-dimension configuration (spatially non-explicit, time varying only), and it reproduced observed median development times without the need for a high-resolution age-stage structure (Hu *et al.*, 2008a) as well as reproduction rates that are consistent with published observations. We generated initial distributions (1 January) from available MARMAP/ECOMON abundance data for 1 December–31 January using objective mapping. As this data set does not include the Scotian Shelf, we complemented it with AZMP (Atlantic Zone Monitoring Program) and CPR data for this upstream region.

The starting point for testing the parameterization was similar to that described by Ji *et al.* (Ji *et al.*, 2009), but included a food-dependence for development (Table I). Food-dependent development was found by

Davis and Alatalo (Davis and Alatalo, 1992) for *C. typicus* in the Gulf of Maine as well as by Klein Breteler *et al.* (Klein Breteler *et al.*, 1995) for *Pseudocalanus elongatus* in the North Sea. The latter further showed that the influence of food on development varies with temperatures (*T*). Ohman and Hsieh (Ohman and Hsieh, 2008) used data from laboratory experiments by Vidal (Vidal, 1980), which likewise showed an increase in generation times of *Calanus pacificus* when food concentration decreased. They present an extended formulation of the temperature-dependent function $D = a \, (T - \alpha)^{-\beta}$ (Belehradek, 1935) for development involving food concentration F (converted from mmol N m^{-3} to µg C L^{-1} using a factor of 79.5):

$$D(T,F) = \frac{a(T - \alpha)^{-\beta}}{1 - \exp(-(qT^s)F)}.$$

This formula, where q describes the influence of food and s represents the change in temperature influence at different food levels, approaches the Belehradek function at high-food concentrations. Parameter values for *C. typicus* are derived from experimental data by Fryd *et al.* (Fryd *et al.*, 1991) for temperature dependence and by Davis and Alatalo (Davis and Alatalo, 1992) for food dependence.

Following Ji *et al.* (Ji *et al.*, 2009), mortality M is simplified as a function of temperature *T*:

$$M(T) = m_0 Q_{10}^{(T - T_0)/10},$$

Table I: Parameter values and life-history traits included as used in different simulations for four model stages eggs (e), nauplii (n), copepodites (c) and adults (a)

	Ji *et al.* (2009)	S0	S1	S2	S3	S4	S5
Development a(e) [d]	921.8	921.8	—	—	—	—	—
Development a(n) [d]	4221.6	4221.6	—	—	—	—	—
Development a(c) [d]	5217.4	5217.4	—	—	—	—	—
Development q(e) [—]	n.d.	1.0	—	—	—	—	—
Development q(n) [—]	n.d.	0.6	—	—	—	—	—
Development q(c) [—]	n.d.	0.4	—	—	—	—	—
Development s(e) [—]	n.d.	0.0	—	—	—	—	—
Development s(n) [—]	n.d.	−0.4	—	—	—	—	—
Development s(c) [—]	n.d.	−1.0	—	—	—	—	—
Development α (°C)	5.3	5.3	—	—	—	—	—
Development β (−)	−2.05	−2.05	—	—	—	—	—
Mortality m_0(e) (d^{-1})	0.150	0.150	0.255	—	—	—	—
Mortality m_0(n) (d^{-1})	0.045	0.045	0.060	—	—	0.065	—
Mortality m_0(c) (d^{-1})	0.020	0.020	0.030	0.035	—	0.045	—
Mortality m_0(a) (d^{-1})	0.030	0.030	0.022	0.030	—	—	—
Mortality Q_{10} (−)	6.00	6.00	1.900	—	—	—	—
Mortality T_0 (°C)	5.00	5.00	—	—	—	—	—
Mortality cannibalism FCT	n.d.	n.d.	—	incl.	—	—	—
Cannibalism critical density K (ind. m^{-3})	n.d.	n.d.	—	750.0	—	—	—
Food source	P	P	—	—	P + Z	—	—
Reproduction r_0 (egg fem^{-1} d^{-1})	93.30	46.63	—	—	—	—	—
Reproduction T_1 (°C)	18.65	18.65	—	—	—	—	—
Reproduction r_1 (°C)	7.62	7.62	—	—	—	—	—
Reproduction k (mg N m^{-3})	1.50	1.50	—	—	—	—	—
Vertical migr FCT	n.d.	n.d.	—	—	—	incl.	—
Vertical migr s_{max} e (ms^{-1})	n.d.	n.d.	—	—	—	0.0	—
Vertical migr s_{max} n (ms^{-1})	n.d.	n.d.	—	—	—	1.0	—
Vertical migr s_{max} c (ms^{-1})	n.d.	n.d.	—	—	—	2.0	—
Vertical migr s_{max} a (ms^{-1})	n.d.	n.d.	—	—	—	2.0	—
Bcond FCT[a]	n.d.	n.d.	—	—	—	—	incl.

[a]Influx was expressed by sine functions as follows:

5–1: BC = 120 · (sin((d − 190)/90) + 1.1) · (sin((d + 50)/45) + 1.1) · tanh(1./z)

5–2: BC = 120 · (sin((d − 190)/90) + 1.1) · (sin((d + 50)/50) + 1.1) · tanh(1./z)

5–3: BC = 120 · (sin((d − 140)/60) + 1.3) · (sin((d + 90)/45) + 1.1) · tanh(1./z)

with a base mortality (m_0) of 0.15 for eggs and lower m_0 of $0.02-0.045$ for the post-hatching stages (Table I) and $Q_{10} = 6$ (at $T_0 = 5$°C). This temperature dependence is used to approximate the combined effects of increased predator populations and predatory consumption rates at higher temperatures and yields mortality rates similar to those obtained from vertical life table (VLT) analysis for C5-adult female *Pseudocalanus* and *C. typicus* on Georges Bank (Ji *et al.*, 2009). Reproduction R is parameterized as a function of temperature T and food F using a Gaussian fit based on observations by Halsband-Lenk *et al.* (Halsband-Lenk *et al.*, 2002) and a Holling-Type III function (Carlotti *et al.*, 2000), respectively:

$$R(T, F) = r_0 \exp - \left[\frac{(T - T_1)^2}{(2r_1^2)}\right] * \frac{F^2}{k^2 + F^2},$$

where r_0 is the maximum egg production rate at temperature T_1, r_1 defines the shape of the curve and k is the half saturation constant for influence of food F. Stage transfer is determined by a probability density function based on the mean-age and the stage duration (Hu *et al.*, 2008a).

$$T(\text{age}) = \min\left(\frac{t_2}{(1 - t_1)}, 1.0\right),$$

where t_1 and t_2 are a cumulative distribution function ("normal_cdf") and a probability density function ("normal_pdf") based on mean-age m and stage duration D using a gradient parameter of $grad_t = 0.4$.

Numerical experiments

Besides these basic processes of development, reproduction, mortality and other life-history strategies are successively included to test the effect and importance of temperature, advection and specific characteristics of *C. typicus* needed to accurately simulate and understand the processes controlling its annual cycle and spatial distribution. As shown in Table I, the aspects examined

include the influence of temperature on mortality (S1), cannibalism and feeding preferences (S2 and S3), active vertical aggregation (S4) and the influence of advection (S5).

We examined the impact of Q_{10}-based temperature-dependent mortality (S1) by reducing the Q_{10} from the value of 6 used in Ji *et al.* (Ji *et al.*, 2009). A lower value of 3 better matches the mortality derived from VLT analysis of the MARMAP/ECOMON data. As shown in the results, an even lower value of 1.9 is required to for the abundance peak to occur during fall.

To assess the impact of cannibalism (S2), we used the findings of Ohman *et al.* (Ohman *et al.*, 2002), who showed increased egg mortality of *C. finmarchicus* at higher female density. They found egg mortality rates to increase linearly to twice the baseline mortality when female abundance is 5000 ind., which exceeds 95% of samples. We added a mortality term for eggs and nauplii that was linearly dependent on the number of adults N_{ad}. Based on the MARMAP/ECOMON data set, the critical value k (95% of data) for *C. typicus* is 750 ind. m^{-3}.

$$M(T, N_{ad}) = M(T) \cdot \left(1 + f(m_i) \cdot \frac{N_{ad}}{K}\right).$$

For the naupliar stages, cannibalism decreased with increasing mean-age m_i by $f(m) = a1/(a1 + m_i)$ consistent with the fact that adults mostly eat younger nauplii. The parameter $a1$ equals two-thirds of the estimated stage duration, i.e. when nauplii reach N4 the cannibalism effect is only 50%. For eggs $f(m)$ equals *1*. Cannibalism was considered as a mortality term only but not as a food source for the females.

In simulations S3 to S5, we examined the potential influence of omnivorous feeding by *C. typicus* on their population dynamics. In these simulations, the food concentration F, which is used in the equations for development and reproduction, was represented by the sum of phytoplankton and microzooplankton concentration from the NPZD model ($F = P + Z$) as opposed to phytoplankton only as in S0–S2 (see Table I).

In the case of S4 and S5 active vertical migration toward the chlorophyll maximum layer z_{chl_max} is included as a hyperbolic function to describe the swimming speed w at each depth layer z in the model:

$$w(z) = w_{max}\tanh[k * (z - z_{chl\_max}) \cdot dz],$$

where $k = 0.02$ is the gradient, w_{max} is the maximum swimming velocity of 1 m h^{-1} for nauplii and 2 m h^{-1} for copepodites/adults (Alcaraz *et al.*, 2007) and dz is the layer thickness. Migration is directed upwards for individuals below the chlorophyll maximum layer

z_{chl_max} and directed downwards for individuals staying above z_{chl_max}. The swimming speed is decreased to zero at the layer of maximum chlorophyll.

We examined the potential influence of the advective influx of *C. typicus* from the Scotian Shelf on the GoM/GB population (S5). In simulations S0–S4, we use a zero-gradient horizontal boundary expression as often used in ecosystem models (Stevens, 1990). Observations of *C. typicus* population abundance from the CPR survey on the Scotian Shelf (Pershing *et al.*, 2010) show an increase in summer and a peak in autumn (Fig. 2a). These observations are similar to data from the AZMP survey (Johnson *et al.*, 2010), which show a strong peak in October. For tests on the influence of advection into the system, we use combined sine functions to approximate the observed seasonal cycle at the upstream end of the model domain. We test three different time series: One strong peak at the end of October fitted to the AZMP data (S5–1), a longer but less strong increase starting in August (S5–2) and the same curve but 1 month earlier (S5–3) to test their influence on the GoM population. In each simulation, the influx is assigned to the five boundary nodes nearest to the coast of Nova Scotia (Fig. 2b). This flux is stronger in the surface (Townsend *et al.*, 2006), and we exponentially decrease the influx v by each layer z with $v = v_{max}/z$ (Fig. 2c).

The impact of each of the above key processes on the seasonal and spatial patterns in *C. typicus* abundance is described in the section 'Results'. We compared simulated annual adult time series to observations in three target areas (Georges Bank, Jordan Basin and Wilkinson Basin), as well as the average modeled bi-monthly spatial distribution on a bi-monthly base, with climatological MARMAP/ECOMON data for 1977–2006 (Fig. 3). The importance of processes for the seasonal cycle and spatial distribution is discussed thereafter. Since the observational data are too sparse for a year-to-year comparison reducing the quality of interpolated spatial plots, climatological data have been found more useful. It is to be noted that in 1999, which is represented in the simulation, *C. typicus* abundances were generally higher than the climatological mean values. All parameter values used in the different simulations are given in Table I.

RESULTS

The annual cycle of *C. typicus* from the baseline model run (S0), as described in Ji *et al.* (Ji *et al.*, 2009, their Fig. 13c/d), is similar to that of *Pseudocalanus* spp., with a peak in early summer, in contrast to the late summer/
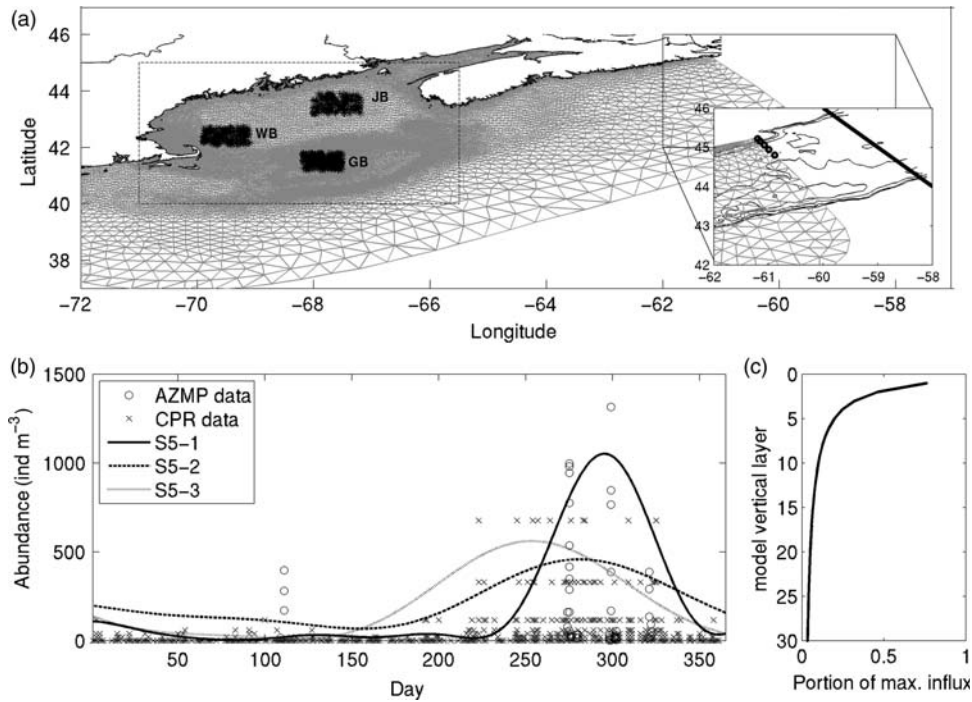
Fig. 2. (**a**) Model grid and positions used for three time series (Figs 5 and 6) located on Georges Bank crest (GB), Jordan Basin (JB) and Wilkinson Basin (WB), subplot: influx was allowed for the five coastal nodes (bold). Indicated is the Louisburg Line of the AZMP data. (**b**) Observed abundances from surveys on the Scotian Shelf (AZMP: Louisburg Line, CPR: all data within subplot of a) and derived sine functions defining boundary conditions in S5−1 to S5−3. (**c**) Influx abundance decreased with each layer z using the factor $1/z$.

autumn peak of *C. typicus* observed in the field (Fig. 3). Higher egg mortality included in the model, to account for broadcast spawning in *C. typicus*, causes an even faster population decline in autumn than for *Pseudocalanus*. While a mortality Q_{10} of 6.0 ($T_0 = 5°C$) fits estimates from the VLT approach using data from Georges Bank (Ji *et al.*, 2009, their Fig. 15), the correlation with temperature using all MARMAP/ECOMON data for GoM/GB is stronger at a lower Q_{10} of 3 at $T_0 = 5°C$ (Fig. 4). However, our tests with $Q_{10} = 3$ still caused the population to go extinct in late summer (not shown). In the following simulations, we therefore further decreased the Q_{10} to 1.9, which causes the Georges Bank population to increase in autumn, but it exceeded observations by more than one order of magnitude (Fig. 5). Furthermore, the populations in the deeper Gulf of Maine regions remained lower than observed, with adult abundance staying <20 ind. m^{-3} (except for a distinct increase in Wilkinson Basin at the end of the year).

To test the effect of density-dependent mortality, cannibalism on eggs and nauplii is included in the succeeding model run (S2). Compared with the simulation S1, this simulation including cannibalism generates a late summer/autumn population peak, which decreases by the end of October (Fig. 5, top panel). In the deeper

basins, the female abundance is low and therefore cannibalism has weaker effect on the population. However, the increase in December in Wilkinson Basin is less than in S1 and adult abundance does not exceed 20 ind. m^{-3} throughout the basins.

Including microzooplankton as an additional food source (S3) does not affect the seasonal timing of the Georges Bank population peak as much as including cannibalism does (Fig. 6). It causes a faster population increase in summer (days 200−260), which results in an overestimation of the population size in August and September. In the deeper GoM basins, the adult abundance is elevated significantly compared with simulation S2. Figure 6 shows an increase from 10 ind. m^{-3} toward 41 ind. m^{-3} in Jordan Basin (+300%) in late October and to 38 ind. m^{-3} in Wilkinson Basin in December, allowing a better agreement with the observed pattern, though observed abundances increase earlier (August) than simulated (September) in both basins.

In summer the maximum phytoplankton concentration in the stratified deeper basins is found 20−30 m below the surface. As a result, rates of development and fecundity are higher in this subsurface layer. The simulation that includes vertical aggregation behavior toward the chlorophyll maximum layer (S4) results in a further increase in depth-averaged abundance in the
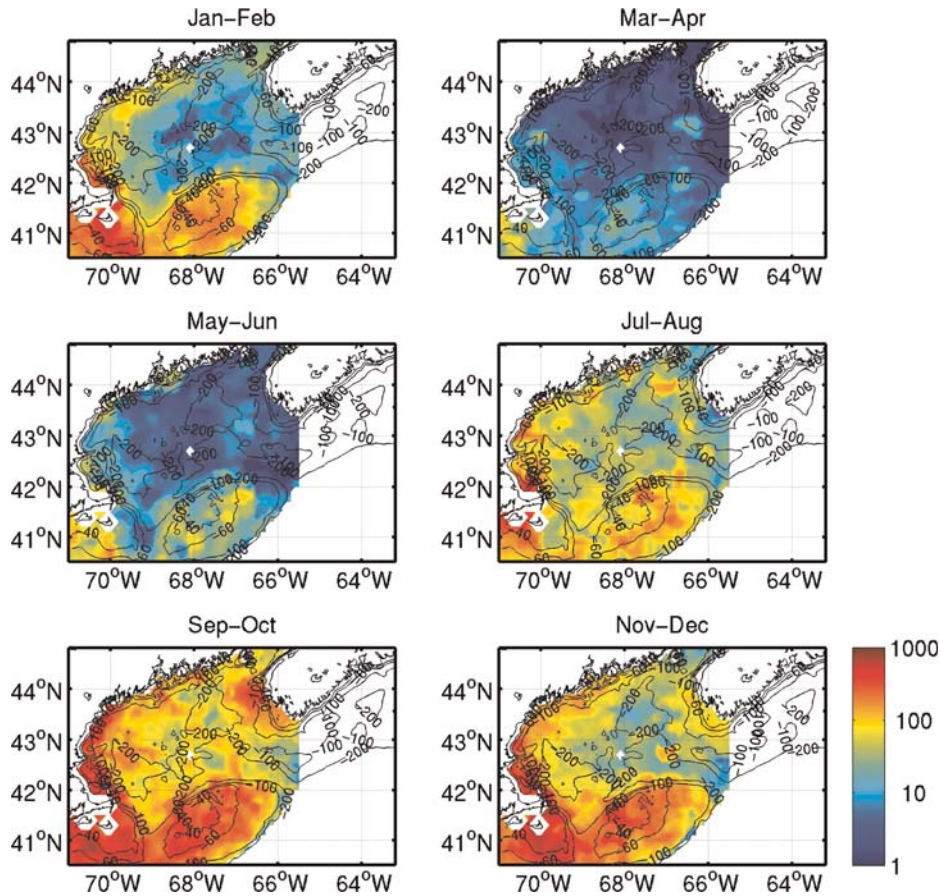
Fig. 3. Bi-monthly abundance distribution of *Centropages typicus* adults from MARMAP/ECOMON as climatology for the years 1977–2006 (vertical average over upper 200 m as ind. m^{-3}).
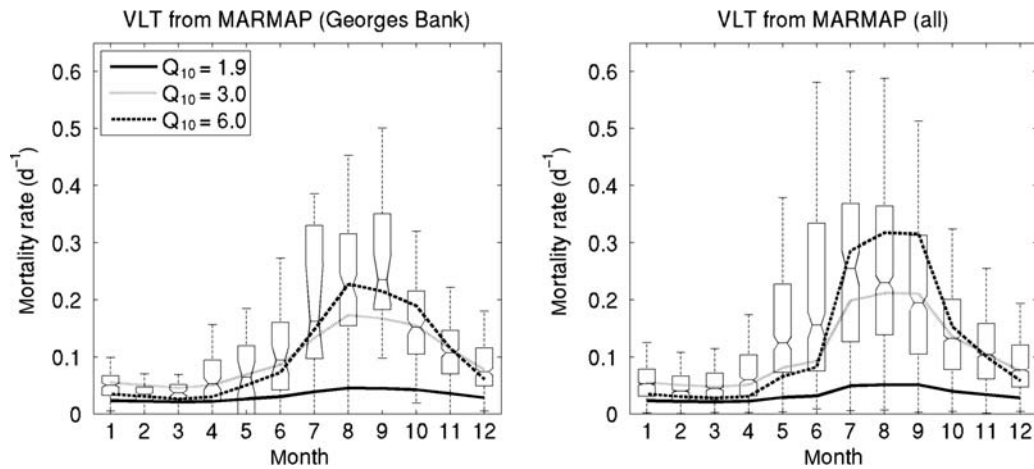

Fig. 4. Monthly averaged mortality rates of *Centropages typicus* CV/adult from MARMAP/ECOMON data using the vertical life table approach (Aksnes and Ohman, 1996) compared with mean mortality rates as Q_{10} function of temperature for two regions: Georges Bank and entire Gulf of Maine/Georges Bank region. Boxplots show median value, 25th and 75th percentile (box) and $1.0 \times$ IQR (inter-quartile range) higher and lower than the quartiles (whiskers).

deeper GoM regions. This influence on the abundance, however, is not as strong as in the simulation that includes microzooplankton as an additional food source (Fig. 6). For the stratified season (given as the mean of May to August), the vertical migration toward the chlorophyll maximum results in an
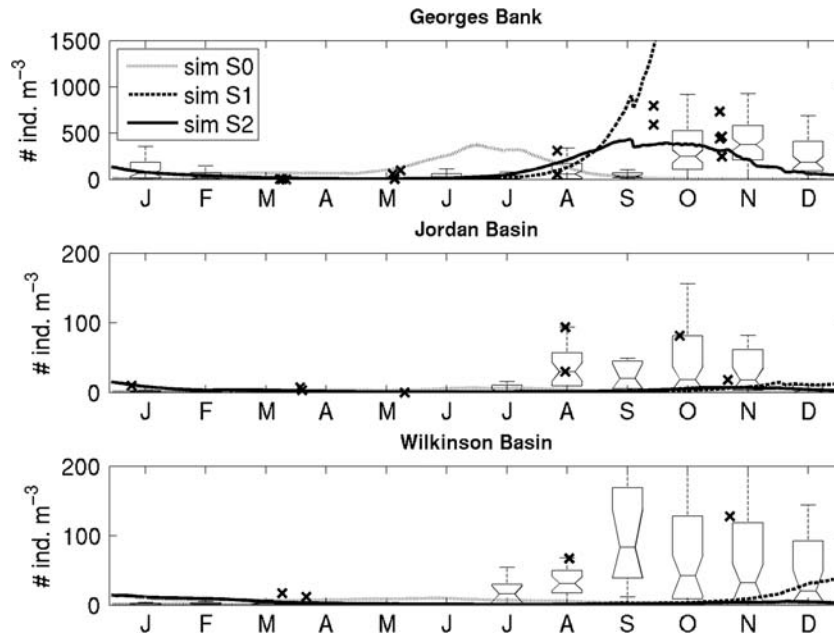
Fig. 5. Time series of daily averaged adult *Centropages typicus* in three regions from simulation with $Q_{10} = 6$ (thin line), with decreased $Q_{10} = 1.9$ (dashed) and including adult cannibalism on young stages (solid thick line) compared with MARMAP/ECOMON data for these areas. Boxplots show the median value, 25th and 75th percentile (box) and $1.0 \times IQR$ higher and lower than the quartiles (whiskers). Both, data and simulation, show average values for the upper 200 m.
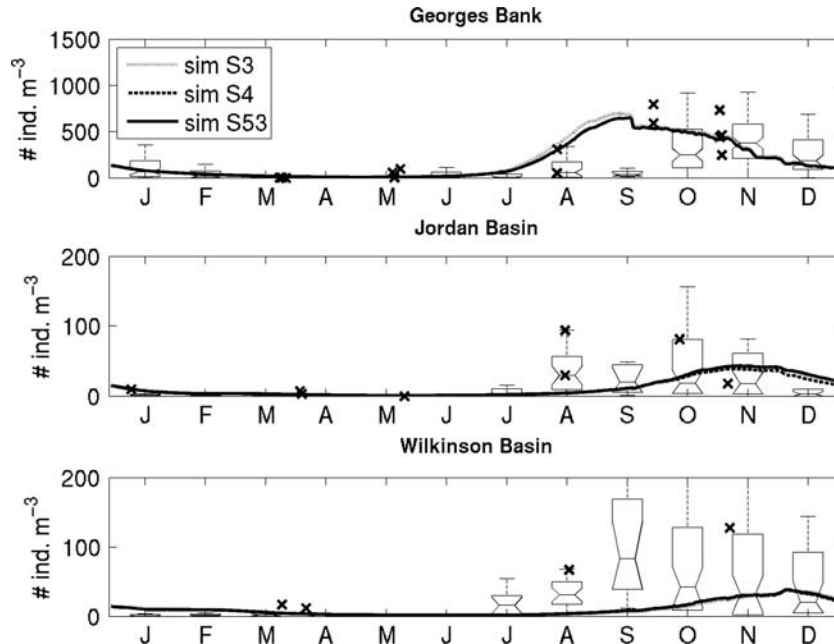

Fig. 6. Time series of daily averaged adult *Centropages typicus* abundance in three regions for simulations including cannibalism and with reproduction and development depending on phytoplankton only (thin line), simulations with a diet of phytoplankton and microzooplankton (dashed line) and adding vertical aggregation (solid thick line). Comparison to data as boxplots as in Fig. 5.

increase in vertically averaged adult abundance by 14% ($1.96-2.29$ ind. m^{-3}) in Jordan Basin and 20% ($2.19-2.75$ ind. m^{-3}) in Wilkinson Basin, while the peak abundance at ~20 m below surface reaches ~13 and 18 ind. m^{-3} for the two stations, respectively

(Fig. 7). This is nearly double that of the surface maximum of 7.5 and 10 ind. m^{-3} found without vertical migration. On the crest of Georges Bank the inclusion of vertical migration has no effect as this area has a vertically homogenous phytoplankton distribution
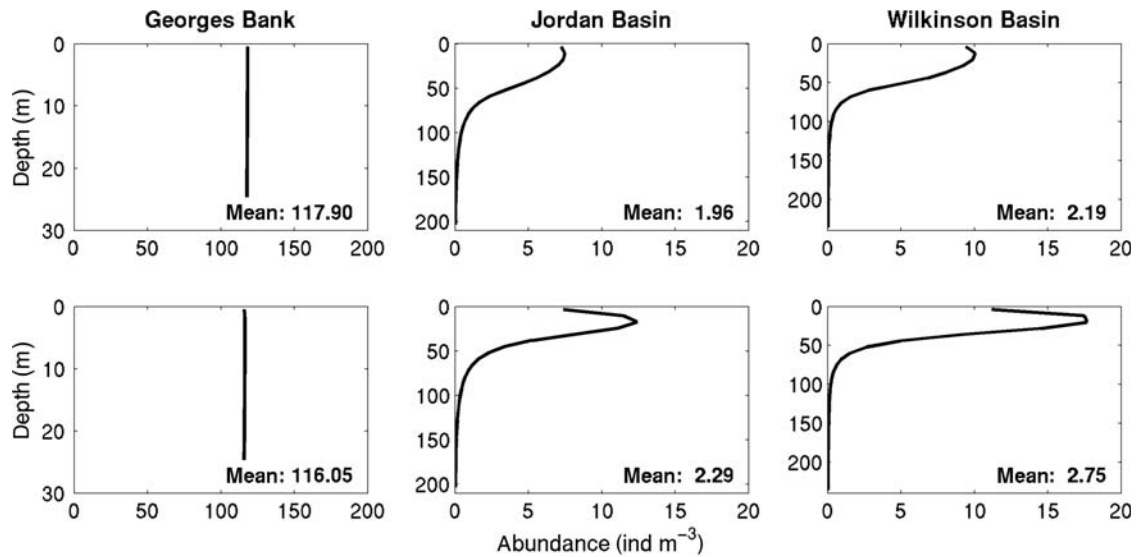
Fig. 7. Vertical profiles of mean adult abundance (ind. m^{-3}) for May to August of *C. typicus* without (upper, S3) and with (lower, S4) vertical migration at three positions: Georges Bank, Jordan Basin and Wilkinson Basin. The vertically average abundance is given as number in each panel.

due to strong tidal mixing throughout the year (Ji *et al.*, 2008a; Hu *et al.*, 2008b).

After incorporating these different life-history strategies (S1–4), the bi-monthly horizontal distribution of vertically averaged *C. typicus* abundance (ind. m^{-3}) shows an overall increase in the central GoM and the basins in the second-half of the year, while the population on Georges Bank decreased in the last 2 months (Fig. 8). These results are similar to observed distributions, while two significant differences remain: First, the population on the Scotian Shelf is extinct by the end of the year, which is not found in observations (Fig. 3). Second, the observed GOM population decreases more quickly in January/February and increases again earlier in July/ August. We tested, whether advection can explain these differences.

The influx at the upstream boundary (Fig. 2) results in an overall increase on the Scotian Shelf in autumn and winter (cf. Figs 8 and 9). The population, which is advected from the NE edge of the Scotian Shelf (west side of Laurentian Channel) toward the GoM, reaches Browns Bank (eastern boundary of the GoM) after ~3 months. The simulation S5–1 with the latest (though strongest) peak does not contribute to the GoM population, since this seasonal pulse of *C. typicus* entering the model area via NE boundary influx is still on the Scotian Shelf when the GoM population decreases. In Jordan Basin the adult abundance decreases compared with simulation S4. In contrast to the strong peak observed from AZMP data, CPR data from the Scotian Shelf reveals an earlier increase in abundance starting in August (Fig. 2). We tested, whether this earlier influx

from the Scotian Shelf can influence the population in the GOM region. This influx could explain the observed abundance increase in Jordan Basin in late summer, which is not simulated in S4 (Fig. 6). Two upstream influxes with increase starting in August (S5–2) and July (S5–3), respectively, are tested. The abundance peak is less strong compared with AZMP data but lasts longer, so that the integrated input abundance is similar. The resulting adult abundance in November/December for these two cases is shown in Fig. 9 (bottom panel). No change was found with the later peak (S5–2), and the abundance peak in November in Jordan Basin was negligible, 41 ind. m^{-3} (S4) to 44 ind. m^{-3} (S5–3). Likewise, the influx had no influence on the population in Wilkinson Basin (Fig. 6). The timing in the seasonal cycle in Jordan Basin also is not changed. This result indicates that the observed increase in September in Jordan Basin is not caused by advection from the Scotian Shelf.

The results of simulation S5–3 show a similar relationship to the temperature-food environment as seen in the observations (Fig. 10 compared with Fig. 1). Highest abundances (copepodites and adults) are found at temperatures of 13–18°C (compared with 10–17°C from observations) significantly decreasing <7°C and over a broad range of chlorophyll. One prominent difference is the high abundance found at 3–4°C and high chlorophyll, which was not found in the observations. This difference is a result of overestimated abundances in winter south of Massachusetts. The highest abundances are found in the same salinity range of 32–33.5 as in the observations.
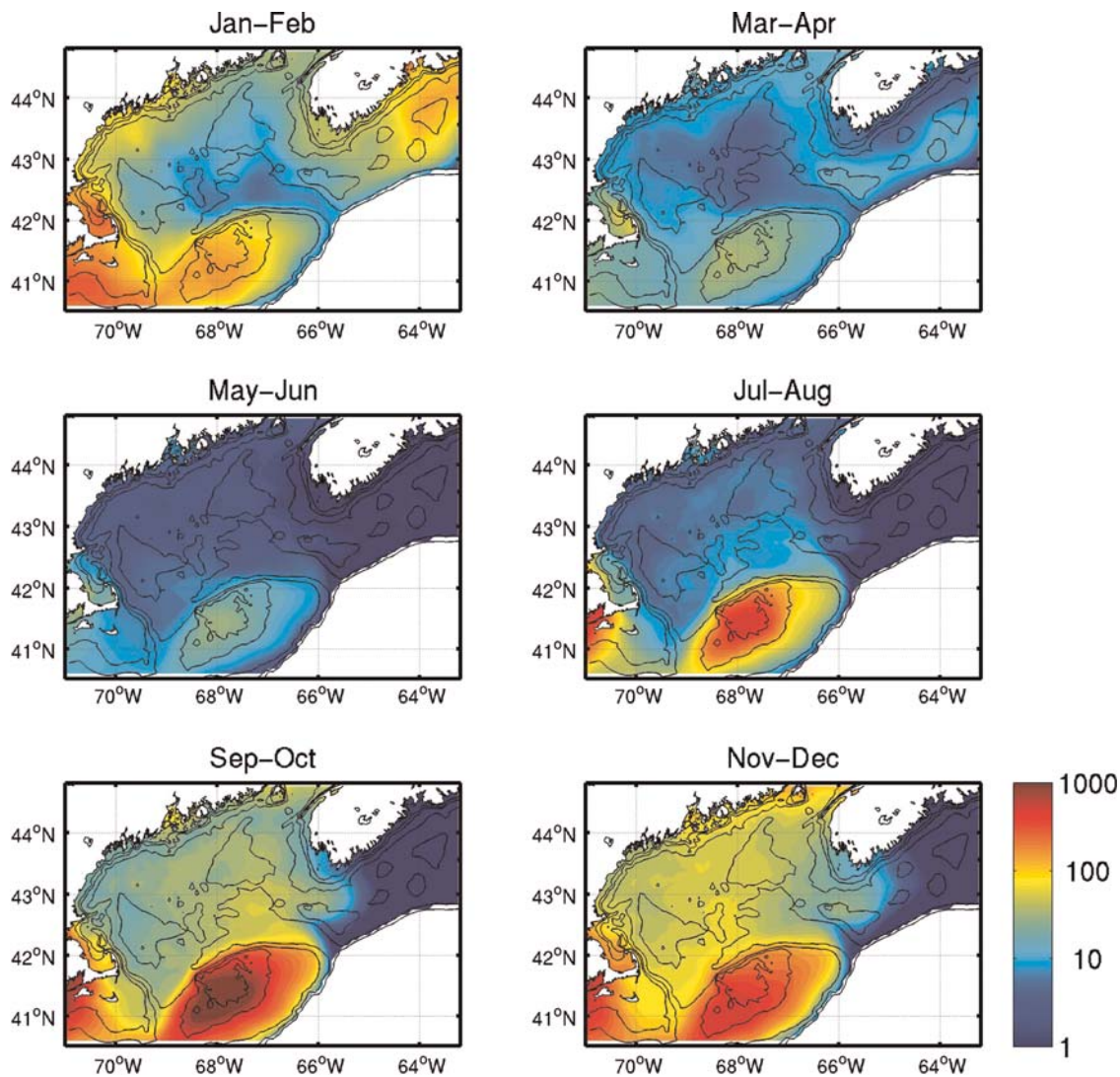
Fig. 8. Bi-monthly simulated *Centropages typicus* adult abundance (vertically averaged ind. m^{-3}) in the model domain when the copepods feed on multiple prey types and move vertically to high prey region (S4).

DISCUSSION

From observations, we find that *C. typicus* can survive low summer food conditions in the surface layers overlying the basins. There also seems to be a constraint on Georges Bank causing the abundance to decline in December, which could not be represented using the temperature-dependent function. This decline happens earlier in the deeper areas. Neither finding is reproduced by the base-run S0 following Ji *et al.* (Ji *et al.*, 2009). To address these two phenomena, we added three life-history strategies reported for *C. typicus*: cannibalism (Davis and Alatalo, 1992), omnivorous feeding (Calbet *et al.*, 2007) and vertical migration (Clarke, 1933; Alcaraz *et al.*, 2007). In the following sections, we discuss these strategies and compare their importance

with biological (food web) and physical (advection) influences.

Mechanisms controlling *C. typicus* population size on Georges Bank

In the population model, we used a temperature-dependent mortality term for all stages. For Georges Bank, a higher Q_{10} ($Q_{10} = 6$ used in run S0) leads to a population decrease in autumn (much earlier than observed), while the lower temperature impact ($Q_{10} = 1.9$) results in an unrealistic increase in population size as shown in run S1. No physiological limitation could be indicated, as temperatures are near the physiological optimum of $16-18°C$ (Calbet *et al.*, 2007) and food is
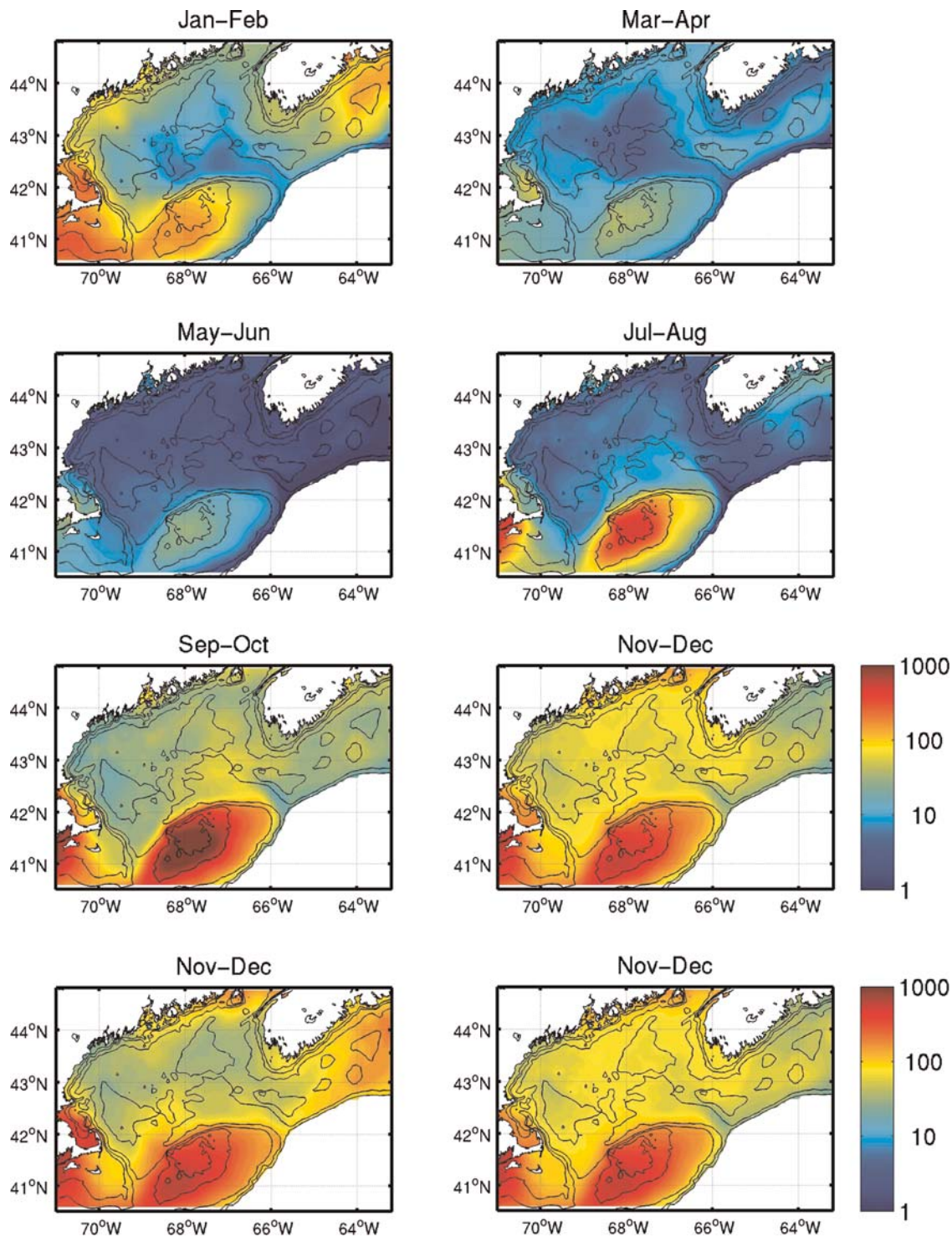
Fig. 9. Top three rows: Bi-monthly simulated *Centropages typicus* adult abundance distribution in the Gulf of Maine as in Fig. 8 but including upstream influx (simulation S5−1). Lower panels: Nov/Dec mean abundance from simulations S5−2 (left) and S5−3 (right) with different upstream influx (see text).

generally not limiting on Georges Bank (Davis, 1984a). That suggests a predatory control of the GB population, as was found for other genera on Georges Bank (*Calanus,*

Pseudocalanus, Paracalanus) (Davis, 1984a, b). However, observations from the MARMAP/ECOMON data set show highest abundance of Chaetognaths, a major
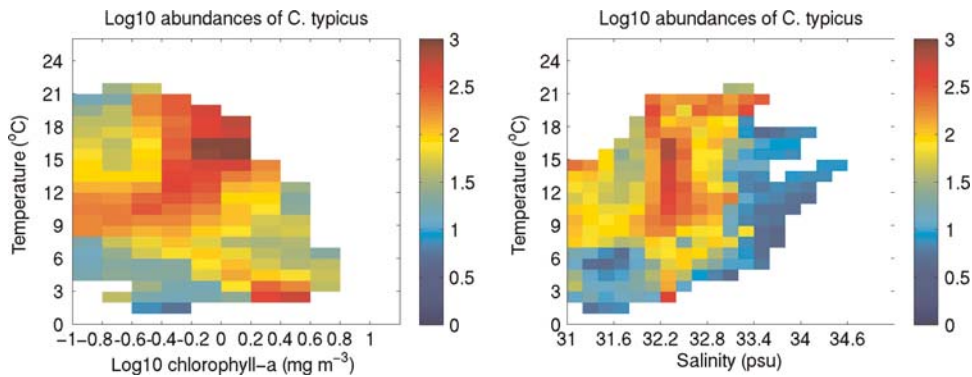
Fig. 10. Simulated abundance (copepodite + adult) of *Centropages typicus* in the Gulf of Maine/Georges Bank region in relation to environmental characteristics. Left: temperature and chlorophyll-*a* concentration, right: temperature and salinity. Coloured abundances are in Log_{10} ind. m^{-3}. Data from gridded simulation results every 5 days on the shelf (depth <400 m) in the area indicated by the dashed rectangle in Fig. 2.
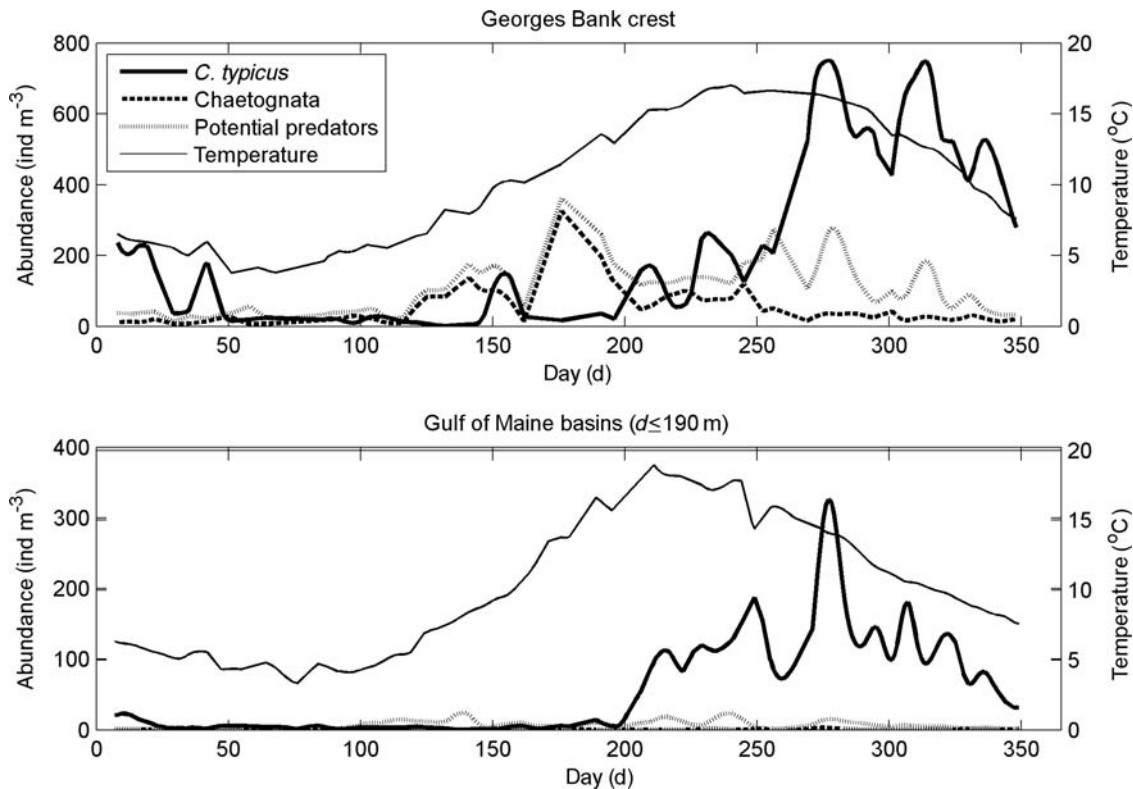

Fig. 11. Observed abundances from MARMAP/ECOMON data set 1977–2006 of *Centropages typicus*, chaetognaths (a primary predator of *C. typicus*) and the sum of potential predators (see text for list) as ind. m^{-3} as mean for two regions: Georges Bank crest and Gulf of Maine basins (≤190 m). Temperature is given for both areas.

predator of *Centropages*, in summer (Fig. 11, upper panel). Abundances of other common predators (incl. Gammaridae, Hyperiidae and Euphausiids) remain high until September, but are low at the time when *C. typicus* decreases. These findings suggest that interspecific predation is not causing the *C. typicus* decrease on Georges Bank. We therefore consider intraspecific predation (cannibalism) as a possible constraint.

Davis and Alatalo (Davis and Alatalo, 1992) emphasized the need to consider cannibalism in experiments with broadcast spawners like *C. typicus*, while experiments of Miralto *et al.* (Miralto *et al.*, 1996) showed that high female density has an impact on female fecundity itself. They also considered that predation is also related to other co-occurring copepod species. In fact, Sell *et al.* (Sell *et al.*, 2001) observed feeding on eggs of *Calanus* by

elder *C. typicus* copepodites. These studies reveal the diversity of processes that can influence copepod mortality. In the present study, we consider only a single species. Carlotti and Slagstad (Carlotti and Slagstad, 1997) examined both the large *Calanus hyperboreus* and the small *Oithona similis* and found that inter-species predation affects both species: by reducing the abundance of *Oithona* the grazing pressure on phytoplankton decreased, which resulted in more food for the slower growing *Calanus*. Though several studies on copepod predation within and between species exist (Bonnet *et al.*, 2004) the effects on the food web are not yet fully understood.

Population maintenance under low-food conditions in the GoM basins

In contrast to cold water species (e.g. *Pseudocalanus* sp.), the abundance of *C. typicus* is low during the spring phytoplankton bloom, but increases from mid-summer to autumn when food levels are lower. Increasing population size at low food levels can be attained either by less mortality, lower metabolic needs or higher efficiency of ingestion or growth. We first look at the possible effect of predation mortality: The average annual abundance of potential predators is lower in deeper regions of the GoM (i.e. where the bottom depth is >150 m) than in shallower regions such as Georges Bank (Fig. 10). In both areas, deep and shallow, the abundance of these predators is highest from May through autumn, during which the *C. typicus* population grows to its annual peak. Based on predator abundance alone, predation pressure would be highest when *C. typicus* abundance is increasing, so decreased mortality is not a likely explanation for its seasonal population growth in summer. Furthermore, for *C. typicus*, no change in metabolism is reported that would decrease its energy expenditure, as for example diapause in *C. finmarchicus* or resting eggs in *C. hamatus* (Durbin and Casas, 2006). In fact, the increasing temperature increases its metabolic needs. Davis and Alatalo (Davis and Alatalo, 1992) found delayed development and growth at food concentrations <2 mg Chl m^{-3}. Thus, based on depth-averaged chlorophyll levels, food limitation is occurring, together with increasing metabolic costs (due to rising temperature) during the period of seasonal population increase.

We examined two possible strategies that could increase *C. typicus* consumption rate: Omnivorous feeding and vertical migration into the chlorophyll maximum layer. *Centropages typicus* is known to feed on a broader food source than expressed in the simplified approach often used in population models (i.e. copepods feeding on phytoplankton) (Calbet *et al.*, 2007). Comparing different dominant copepod species in the

GoM revealed that omnivorous feeding is found primarily in the warm water species. Omnivory was reported for *Oithona* sp. (Gonzalez and Smetacek, 1994) as well as for *Paracalanus* sp. (Mauchline, 1998), both of are found at highest abundance in October to November (Davis, 1987). In contrast, species considered to be herbivorous like *C. finmarchicus*, *Pseudocalanus* sp. or *Acartia* sp. (Mauchline, 1998 and references therein) have a dominant peak in spring, coinciding with the spring diatom bloom in the GoM/GB region. The model tests presented in this paper suggest that omnivorous feeding is a requirement for *C. typicus* to build higher abundances in the autumn.

Though copepods are often assumed to be passively drifting within the water, there have been several experiments on copepod swimming behavior as reviewed by Alcaraz *et al*. (Alcaraz *et al.*, 2007). Vertical movement is usually reported as diel vertical migration (Hays, 2003) or seasonal migration for diapause (Thorisson, 2006), strategies basically to avoid predation in the illuminated upper layer. Vertical movement by copepods may also improve copepod nutrition: Observations indicate that *C. typicus* is capable of perceiving its ambient food conditions (Poulet and Gill, 1988; Jackson and Kiørboe, 2004) and adjusts its swimming behavior toward a more favorable place. One constraint is the increased density reducing fecundity and Miralto *et al.* (Miralto *et al.*, 1996) raise the question about the trade-off between increased fecundity and increased predation loss through cannibalism. However, considering a temperature of ∼12°C in early summer the increased female abundance at the chlorophyll maximum layer (Fig. 7) would raise the egg mortality rate only by 1–2%, so that crowding is not an issue in the GOM, where abundances are low.

Influence of upstream advective input on the GoM population

The GoM/GB region is a highly advective system, with the major current system entering the Eastern Scotian Shelf before reaching the GoM and leaving through the Great South Channel (Mountain, 2004; Townsend *et al.*, 2006). While omnivorous feeding and vertical migration help the population in the deeper areas to increase further compared with the (simple) basic parameterization, the population on the Scotian Shelf is not able to survive unless fueled by an upstream influx, and the GoM population are diluted and eventually depleted if this situation continues. The upstream source of *C. typicus* is thus critically important for the persistence of the observed high population abundance on the Scotian Shelf. As *C. typicus* is usually not found in

deeper waters off the shelves (Durbin and Kane, 2007), the slope area is not likely to be a source contributing to maintain the GOM/GB population. Observations from the AZMP survey show only a few *C. typicus* in the southwestern part of the Gulf of Saint Lawrence (Johnson *et al.*, 2010). However, the hydrographic conditions for the southeastern part (temperature up to $17.5°C$ in summer) suggest that this species is capable of surviving in this region. Herman *et al.* (Herman *et al.*, 1991) found that the Nova Scotia Current is a dominant supplier of *Calanus* sp. but also smaller copepods from the Gulf of St Lawrence to the Scotian Shelf. The source of high abundances on the Scotian shelf could be a combination of *in situ* growth and some supply from upstream. Further investigation is needed to identify the exact cause.

Our model results showed that information beyond the model domain is important and the definition of correct boundary conditions can be crucial to the simulation. The Gulf of Maine is situated in between different ecosystems (Gulf of St Lawrence in the north and the Middle Atlantic Bight in the south), which are connected by the current system. One solution would be an extension of the model domain. However, inter-regional modeling applications are challenging due to possible regional adaptation of copepods to the environment (Halsband-Lenk *et al.*, 2002).

A note on parameter sensitivity

While the process formulations of development and reproduction are based on experimental data and considered robust, other parameters are difficult or impossible to estimate from observations and the influence on the annual cycle is unclear. These uncertainties include the formulations for transfer through life stages, the upstream boundary condition, vertical migration and the mortality. In the results, we showed the effect of different formulations for the upstream influx on the Scotian Shelf. Further simulations focused on the effects of the transfer gradient ($grad_t$), the condition for vertical migration as well as mortality parameters (Q_{10} and base mortality). Tests on the sensitivity of these parameters in terms of timing and magnitude of abundances in two regions (Georges Bank and Jordan Basin) confirmed that the greatest sensitivity was to mortality (Fig. 12), as was found by Ji *et al.* (Ji *et al.*, 2009).

Using a lower value for $grad_t$, i.e. a stronger gradient for individuals to be transferred from one stage to the next, did not affect the timing of the abundance peak and number of adults on Georges Bank were reduced by ~10% at the stronger gradient. This can be explained by individuals staying longer in a stage,

which has a higher mortality rate than the following. However, there was no effect in the basin. We further compared the simulation including omnivorous feeding ($S-3$) against a case including vertical migration but without omnivorous behavior. This showed the stronger effect of omnivory on population size compared with vertical migration. While the addition of vertical migration only resulted in an population increase in ~30% in Jordan Basin and had no effect on Georges Bank, the simulation with omnivorous feeding resulted in a population increase in two times and five times on Georges Bank and in Jordan Basin, respectively. This is caused by the higher amount of microzooplankton in the upper layers compared with the surplus of food found at the chlorophyll maximum layer. Including cannibalism on nauplii changed the timing of the peak by $3-4$ weeks in October to November, when adults were more abundant, while generally abundances decreased by ~40% compared with cannibalism on eggs only. Changing the age limit for cannibalism within the naupliar stages had much less impact on the abundances.

The strongest influence, however, was found with a change in mortality rates. The change in Q_{10} is shown in Fig. 5 resulting in a shift of abundance peak from summer to autumn. Reducing the Q_{10} by 10% ($1.9 \rightarrow 1.7$) resulted in lower abundance on Georges Bank (-30%), while in Jordan Basin maximum adult abundance was 2.5 times higher. Both sites experienced a shift of the peak of ~1 month. Changes in the base mortality, however, did not have any effect on the abundance timing. An increase in 20% in egg base mortality and 10% in nauplii and copepodite mortality resulted in a mean decrease in ~50% of the peak abundance. These strong changes due to changes in the mortality parameters suggest the need for further investigation of representation of mortality in copepod population models.

A note on mortality

Observations reveal a correlation between mortality rates and temperature (Fig. 3). Thus, temperature is often used as a proxy for mortality assumed to come from predation. Ji *et al.* (Ji *et al.*, 2009) showed good agreement of calculated mortality rates from observations on Georges Bank and a temperature-based function using a Q_{10} of 6.0 ($T_0 = 5°C$). Their simulated monthly mortalities are similar to observations using the VLT approach. For our simulation including *C. typicus* a calculated Q_{10} of 3.0 caused the population to go extinct. However, if we use VLT to calculate the copepodite mortality from model simulated abundances (not observational data), the instant mortality rate in the
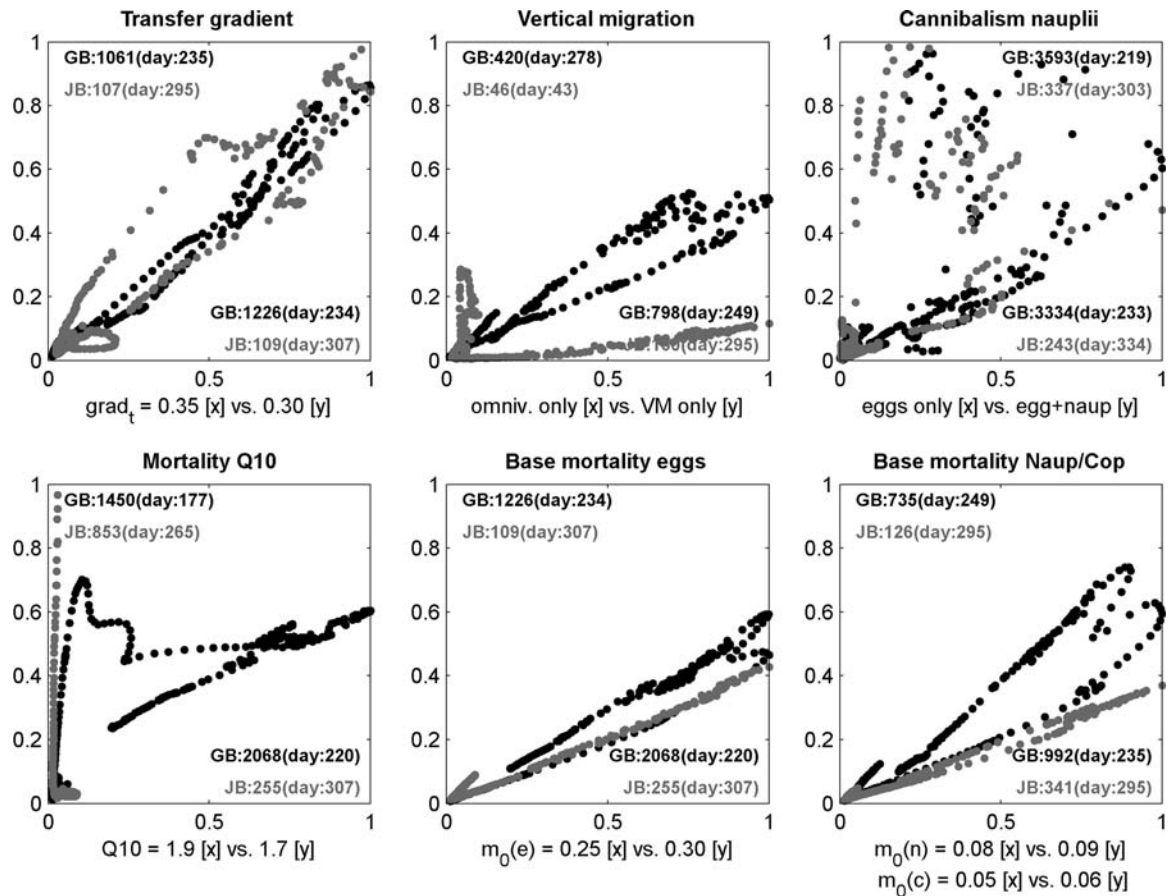
Fig. 12. Sensitivity tests for different parameters: Comparison of time series at two stations [Georges Bank (black) and Jordan Basin (gray)] from two simulations, where a single parameter value was changed. Adult abundances from simulations using the first (*x*-axis) case in the axis label are opposed to the second (*y*-axis) case (abundances have been normalized by the maximum value of both simulations together to better compare the two regions). Peak abundance and peak day in brackets are given for each simulation and region (first case in the label given in lower right side).

second-half of the year is comparable with the Q_{10} of 3.0, although a lower Q_{10} of 1.9 is used in the model parameterization, suggesting a mismatch between the VLT-derived mortality and model-specified mortality possibly due to the strong assumption made in the VLT approach (Aksnes and Ohman, 1996).

A further note considers the use of temperature as a proxy for predation. This method works well to describe decreased abundances in cold water species, e.g. *Pseudocalanus* (Ji *et al.*, 2009) or *Calanus* (Plourde *et al.*, 2009). However, for *C. typicus* this is not the case as described earlier. Highest predator abundances are found earlier than the temperature maximum and at a stronger gradient than surface temperatures indicate (Fig. 10). Additional tests with a spatially inhomogeneous mortality rate (using microzooplankton as a proxy for food conditions and thus higher predator abundance) are able to simulate observed differences in

the timing of *C. typicus*: an earlier increase in the GoM basins due to lower mortality and a later increase on Georges Bank, where predator abundance is much higher. On the contrary, this formulation underestimates mortality rates in winter when microzooplankton concentrations are very low. One possible reason for the mismatch of predators and mortality rates could be the representation of potential predators as, for example, gelatinous zooplankton are considered important grazers of copepods but are not represented in our data set. This indicates the necessity for a more precise description of predation for some species.

CONCLUSION

To estimate the role of *C. typicus* in the ecosystem, it is necessary to understand their species-specific dynamics

and to know which processes are important in their life strategies. This paper focuses on several processes generally not included in simplified copepod population models and their contribution to the spatio-temporal distribution. We showed that cannibalism and omnivorous feeding are potentially important aspects in the life-history strategy of *C. typicus* as they can influence the seasonal dynamics in different areas of the Gulf of Maine system. This highlights the need to understand relevant life-history traits for modeling specific copepod populations. We also show that the regional plankton changes are related to upstream conditions, which requires information on a larger spatial domain.

ACKNOWLEDGEMENTS

FUNDING

APPENDIX: THE BIOLOGICAL MODEL

The lower trophic level model includes inorganic nitrogen, phytoplankton, zooplankton and detritus (NPZD) and describes the basic nitrogen cycle in the system. The model has been described fully in our early publication (Ji *et al.*, 2008a, b). Below is a brief summary of the model structure and equations. The model includes the uptake of inorganic nitrogen by phytoplankton $(\mathcal{N} \to P)$, grazing by zooplankton $(P \to \mathcal{Z})$ and excretion $(P \to \mathcal{N})$ as well as (particulate) plankton loss $(P \to D; \mathcal{Z} \to D)$, which sinks toward the sea floor (detritus). The pathway for the remineralization of organic particles is $D \to \mathcal{N}$. The set of biological equations are:

$$\frac{\mathrm{d}\mathcal{N}}{\mathrm{d}t} = -1.5\frac{\mathcal{N}}{0.5+\mathcal{N}}\cdot fI \cdot 2^{\frac{(T-10)}{10}}P \quad +0.3\left[0.3\frac{P^2}{0.5^2+P^2}2.5^{\frac{(T-10)}{10}}\right]\mathcal{Z} \quad +0.06\cdot 2^{\frac{(T-10)}{10}}D$$

$$\frac{\mathrm{d}P}{\mathrm{d}t} = 1.5\frac{\mathcal{N}}{0.5+\mathcal{N}}\cdot fI \cdot 2^{\frac{(T-10)}{10}}P \quad -0.3\frac{P^2}{0.5^2+P^2}2.5^{\frac{(T-10)}{10}}\mathcal{Z} \quad -0.1\cdot 2^{\frac{(T-10)}{10}}P$$

$$\frac{\mathrm{d}\mathcal{Z}}{\mathrm{d}t} = +0.3\left[0.3\frac{P^2}{0.5^2+P^2}2.5^{\frac{(T-10)}{10}}\right]\mathcal{Z} \quad -0.2\cdot 2.5^{\frac{(T-10)}{10}}\mathcal{Z}^2$$

$$\frac{\mathrm{d}D}{\mathrm{d}t} = +0.4\left[0.3\frac{P^2}{0.5^2+P^2}2.5^{\frac{(T-10)}{10}}\right]\mathcal{Z} \quad +0.1\cdot 2^{\frac{(T-10)}{10}}P \quad +0.2\cdot 2.5^{\frac{(T-10)}{10}}\mathcal{Z}^2 \quad -0.06\cdot 2^{\frac{(T-10)}{10}}D$$

| nutrient_uptake | grazing | phyto_loss | zoo_loss | remineralization |

In this model parameter, values for zooplankton are chosen to resemble microzooplankton. fI describes the influence of light on phytoplankton uptake with $fI = (1 - \mathrm{e}^{-0.025 \cdot I})\cdot \mathrm{e}^{-0.001 \cdot I}$. Sinking velocities are 1 and 10 ms^{-1} for phytoplankton and detritus, respectively.

REFERENCES

Aksnes, D. L. and Ohman, M. D. (1996) A vertical life table approach to zooplankton mortality estimation. *Limnol. Oceanogr.*, **41**, 1461–1469.

Alcaraz, M., Saiz, E. and Calbet, A. (2007) *Centropages* behaviour: swimming and vertical migration. *Progr. Oceanogr.*, **72**, 121–126.

Beaugrand, G., Lindley, J. A., Helaouet, P. *et al.* (2007) Macroecological study of *Centropages typicus* in the North Atlantic Ocean. *Progr. Oceanogr.*, **72**, 259–273.

Belehradek, J. (1935) *Temperature and Living Matter.* Bornträger, Berlin, 71pp.

Bonnet, D., Titelman, J. and Harris, R. (2004) Calanus the cannibal. *J. Plankton Res.*, **26**, 937–948.

Calbet, A., Carlotti, F. and Gaudy, R. (2007) The feeding ecology of the copepod *Centropages typicus* (Krøyer). *Progr. Oceanogr. B.*, **72**, 137–150.

Carlotti, F. and Slagstad, D. (1997) Population dynamics model of interacting copepod species coupled with a 1-D model of

phytoplankton dynamics in the Greenland Sea Gyre. *Environ. Model. Assess.*, **2**, 29–36.

Carlotti, J., Giske, J. and Werner, F. (2000) Modeling zooplankton dynamics. In: Harris, R., Wiebe, P., Lenz, J., Skjoldal, H. -R. and Huntley, M. (eds), *ICES Zooplankton Methodology Manual*. Academic Press, London, pp. 571–667.

Chen, C., Huang, H., Beardsley, R. C. *et al*. (2007) A finite-volume numerical approach for coastal ocean circulation studies: comparison with finite difference models. *J. Geophys. Res.*, **112**, C03018. doi:10.1029/2006JC003485.

Chen, C. S., Liu, H. D. and Beardsley, R. C. (2003) An unstructured grid, finite-volume, three-dimensional, primitive equations ocean model: application to coastal ocean and estuaries. *J. Atm. Ocean. Tech.*, **20**, 159–186.

Clarke, G. L. (1933) Diurnal migrations of plankton in the Gulf of Maine and its correlation with changes in submarine irradiation. *Biol. Bull.*, **65**, 402–436.

Continuous Plankton Recorder Survey Team (2004) Continuous plankton records: plankton atlas of the north atlantic Ocean (1958–1999). *Mar. Ecol. Progr. Ser.*, (Suppl.), 1–75. http://www.int-res.com/journals/meps/

Davis, C. S. (1984a) Food concentrations on Georges Bank: non-limiting effect on growth and survival of laboratory reared *Pseudocalanus sp* and *Paracalanus parvus*. *Mar. Biol.*, **82**, 42–46.

Davis, C. S. (1984b) Predatory control of copepod seasonal cycles on Georges Bank. *Mar. Biol.*, **82**, 31–40.

Davis, C. S. (1987) Zooplankton life cycles. In: Backus, R. H. and Bourne, D. W. (eds), *Georges Bank*. MIT Press, Cambridge, MA, pp. 256–267.

Davis, C. S. and Alatalo, P. (1992) Effects of constant and intermittent food-supply on life-history parameters in a marine copepod. *Limnol. Oceanogr.*, **37**, 1618–1639.

Durbin, E. G. and Casas, M. C. (2006) Abundance and spatial distribution of copepods on Georges Bank during the winter/spring period. *Deep-Sea Res. II.*, **53**, 2537–2569.

Durbin, E. and Kane, J. (2007) Seasonal and spatial dynamics of *Centropages typicus* in the western North Atlantic. *Progr. Oceanogr.*, **72**, 249–258.

Fryd, M., Haslund, O. H. and Wohlgemuth, O. (1991) Development, growth and egg production of the two copepod species *Centropages hamatus* and *Centropages typicus* in the laboratory. *J. Plankton Res.*, **13**, 683–689.

Gonzalez, H. E. and Smetacek, V. (1994) The possible role of the cyclopoid copepod *Oithona* in retarting vertical flux of zooplankton faecal material. *Mar. Ecol. Progr. Ser.*, **113**, 233–246.

Halsband-Lenk, C., Hirche, H. J. and Carlotti, F. (2002) Temperature impact on reproduction and development of congener copepod populations. *J. Exp. Mar. Biol. Ecol.*, **271**, 121–153.

Hays, G. C. (2003) A review of the adaptive significance and ecosystem consequences of zooplankton diel vertical migrations. *Hydrobiol.*, **503**, 163–170.

Herman, A. W., Sameoto, D. D., Shunnian, C. *et al*. (1991) Sources of zooplankton on the Nova Scotian Shelf and their aggregations within deep-shelf basins. *Cont. Shelf Res.*, **11**, 211–238.

Hu, Q., Davis, C. S. and Petrik, C. M. (2008a) A simplified age-stage model for copepod population dynamics. *Mar. Ecol. Progr. Ser.*, **360**, 179–187.

Hu, S., Townsend, D. W., Chen, C. *et al*. (2008b) Tidal pumping and nutrient fluxes on Georges Bank: a process-oriented modeling study. *J. Mar. Sys.*, **74**, 528–544.

Jackson, G. A. and Kiørboe, T. (2004) Zooplankton use of chemodetection to find and eat particles. *Mar. Ecol. Progr. Ser.*, **269**, 153–162.

Ji, R., Davis, C. S., Chen, C. *et al*. (2008a) Influence of local and external processes on the annual nitrogen cycle and primary productivity on Georges Bank: a 3-D biological-physical modeling study. *J. Mar. Sys.*, **73**, 31–47.

Ji, R., Davis, C. S., Chen, C. *et al*. (2008b) Modeling the influence of low-salinity water inflow on winter-spring phytoplankton dynamics in the Nova Scotian Shelf-Gulf of Maine region. *J. Plankton Res.*, **30**, 1399–1416.

Ji, R. B., Davis, C. S., Chen, C. S. *et al*. (2009) Life history traits and spatio-temporal distributional patterns of copepod populations in the Gulf of Maine-Georges Bank region. *Mar. Ecol. Progr. Ser.*, **384**, 187–205.

Johnson, C., Curtis, A., Pepin, P. *et al*. (2010) Spatial patterns in zooplankton communities and their seasonal variability in the northwest Atlantic. *AZMP Bull.*, **9**, 27–32.

Kane, J. (2007) Zooplankton abundance trends on Georges Bank, 1977–2004. *ICES J. Mar. Sci.*, **64**, 909–919.

Kiørboe, T. (2008) Optimal swimming strategies in mate-searching pelagic copepods. *Oecologia.*, **155**, 179–192.

Klein Breteler, W. C. M., Gonzales, S. R. and Schogt, N. (1995) Development of *Pseudocalanus elongatus* (Copepoda, Calanoida) cultured at different temperature and food conditions. *Mar. Ecol. Progr. Ser.*, **119**, 99–110.

Lough, R. G., Buckley, L. J., Werner, F. E. *et al*. (2005) A general biophysical model of larval cod (*Gadus morhua*) growth applied to populations on Georges Bank. *Fish. Oceanogr.*, **14**, 241–262.

Mauchline, J. (1998) The biology of calanoid copepods. *Adv. Mar. Biol.*, **33**, 710.

Miralto, A., Ianora, A., Poulet, S. A. *et al*. (1996) Is fecundity modified by crowding in the copepod *Centropages typicus*? *J. Plankton Res.*, **18**, 1033–1040.

Mountain, D. G. (2004) Variability of the water properties in NAFO subareas 5 and 6 during the 1990s. *J Northwest Atl. Fish. Sc.*, **34**, 103–112.

Niehoff, B. (2007) Life history strategies in zooplankton communities: the significance of female gonad morphology and maturation types for the reproductive biology of marine calanoid copepods. *Progr Oceanogr.*, **74**, 1–47.

Ohman, M. D. and Hsieh, C. H. (2008) Spatial differences in mortality of *Calanus pacificus* within the California current system. *J. Plankton Res.*, **30**, 359–366.

Ohman, M. D., Runge, J. A., Durbin, E. G. *et al*. (2002) On birth and death in the sea. *Hydrobiol.*, **480**, 55–68.

Pershing, A. J., Head, E. J. H., Greene, C. H. *et al*. (2010) Pattern and scale of variability among northwest Atlantic Shelf plankton communities. *J. Plankton Res.*, **32**, 1661–1674.

Peterson, W. T. (2001) Patterns in stage duration and development among marine and freshwater calanoid and cyclopoid copepods: a review of rules, physiological constraints, and evolutionary significance. *Hydrobiol.*, **453**, 91–105.

Plourde, S., Maps, F. and Joly, P. (2009) Mortality and survival in early stages control survival in *Calanus finmarchicus*. *J. Plankton Res.*, **31**, 371–388.

Poulet, S. A. and Gill, C. W. (1988) Spectral analyses of movements made by the cephalic appendages of copepods. *Mar. Ecol. Progr. Ser.*, **43**, 259–267.

Sell, A. F., van Keuren, D. and Madin, L. P. (2001) Predation by omnivorous copepods on early developmental stages of *Calanus finmarchicus* and *Pseudocalanus* spp. *Limnol. Oceanogr.*, **46**, 953–959.

Sherman, K. (1980) MARMAP, a fisheries ecosystem study in the NW Atlantic: fluctuations in the ichthyoplankton–zooplankton components and their potential for impact on the system. In: Diemer, F. P., Vernverg, F. J. and Mirkes, D. Z. (eds.), *Advanced Concepts on Ocean Measurements for Marine Biology.* Belle W. Baruch Institute for Marine Biology and Coastal Res., Univ. South Carolina Press, Columbia, SC, pp. 9–37.

Stevens, D. P. (1990) On open boundary conditions for three dimensional primitive equation ocean circulation models. *Geophys. Astrophys. Fluid Dyn.*, **51**, 103–133.

Thorisson, K. (2006) How are the vertical migrations of copepods controlled? *J. Exp. Mar. Biol. Ecol.*, **329**, 86–100.

Townsend, D. W., Thomas, A. C., Mayer, L. M. *et al.* (2006) *Oceanography of the Northwest Atlantic Continental Shelf.* In: Robinson, A. R. and Brink, K. H. (eds), *The Sea: The Global Coastal Ocean: Interdisciplinary Regional Studies and Syntheses.* Harvard University Press, pp. 119–168.

Vidal, J. (1980) Physioecology of zooplankton. I. Effects of phytoplankton concentration, temperature, and body size on the growth rate of *Calanus pacificus* and Pseudocalanus sp. *Mar. Biol.*, **56**, 111–134.

Voss, R., Dickmann, M. and Schmidt, J. O. (2009) Feeding ecology of sprat (*Sprattus sprattus* L.) and sardine (*Sardina pilchardus* W.) larvae in the German Bight, North Sea. *Oceanologia.*, **51**, 117–138.